Pis'ma v ZhETF, vol. 82, iss. 1, pp. 36 – 40

Magnetic phase transitions in TbNi$_5$ single crystal: bulk properties and neutron diffraction studies

S. Lee^{+}, *A. A. Podlesnyak**, *K. Prokes*$^{\triangle}$, *V. E. Sikolenko*$^{\triangle}$, *A. S. Ermolenko*$^{\square}$, *E. G. Gerasimov*$^{\square}$, *Yu. A. Dorofeev*$^{\square}$, *A. P. Vokhmyanin*$^{\square}$, *J.-G. Park*$^{+\nabla}$, *A. N. Pirogov*$^{+\square}$

$^{+}$*Department of Physics and Institute of Basic Science, SungKyunKwan University, Suwon 440-746, South Korea*

**Laboratory for Neutron Scattering, ETH Zurich & Paul Scherrer Institute, Villigen 5232 PSI, Switzerland*

$^{\triangle}$*BENSC, Hahn-Meitner Institute, Berlin D-14109, Germany*

$^{\square}$*Institute of Metal Physics of RAS, 620219 Ekaterinburg, Russia*

$^{\nabla}$*Center for Strongly Correlated Materials Research, Seoul National University, Seoul 151-742, South Korea*

Submitted 23 May 2005

The magnetic susceptibility, heat capacity and neutron diffraction measurements have been carried out in order to study the unusual magnetic ordering of TbNi$_5$ using a single crystal over the temperature region of 2∼30 K. Two spontaneous magnetic transitions have been observed: one is a second order transition from a paramagnetic state to an incommensurate structure (T_p =24 K) and the other a first order transition from the incommensurate structure to a lock-in phase ($T_f^c = 10$ K). We also found an irreversible magnetic field-induced transition from the modulated structure to the ferromagnetic collinear one.

PACS: 75.25.+z, 75.30.Kz, 61.12.−q

1. Introduction. The exchange interaction and crystal field splitting of rare-earth intermetallic RNi$_5$ compounds have been a subject of great interests largely because of the simple crystal and magnetic structures. Their magnetic properties are determined mainly by rare-earth ions [1]. The rare-earth elements occupy 1a positions of the CaCu$_5$-type lattice ($P6/mmm$ space group) and their magnetic moment values are found to be close to that of the free rare-earth ions. The Ni atoms occupy 2b and 3d positions with its ordered magnetic moments less than $0.2\,\mu_B$. Most of these RNi$_5$ intermetallics have been studied in detail by various experimental methods. Particularly, TbNi$_5$ has been extensively studied using several experimental techiniques: magnetic measurements [2], heat-capacity [3], elastic and inelastic neutron scattering [4 – 6], positive μSR spectroscopy [7] and spin-echo NMR [8] studies. The results of these investigations appeared to be in good agreement with the ferromagnetic model of the magnetic structure and there seemed to be no reason whatsoever to suspect otherwise until quite recently.

However, recent electrical resistance [9], AC susceptibility and magnetization [10, 11] data indicated that the magnetic state of TbNi$_5$ might be more subtle than the proposed simple ferromagnetic structure. According to Ref. [9], the resistance, when measured along the a-axis (the magnetic easy direction), exhibits characteristic behavior for a ferromagnet with Curie temperature $T_C = 23$ K, while that measured along the c axis (the magnetic hard direction) shows an anomalous peak below T_C: these peaks were observed at 17.4 and 21.2 K for cooling and heating curves, respectively. Authors of Refs. [10, 11] also observed anomalies in the temperature and field dependence of their AC susceptibility. For example, the temperature dependence of the AC susceptibility shows two peaks at $T_f = 16.5$ K and $T_p = 23.5$ K. The authors of Ref. 11 then proposed that the TbNi$_5$ compound is a helimagnetic antiferromagnet between T_f and T_p under external magnetic field smaller than $H_c = 0.45$ kOe, and becomes ferromagnetic for $T < T_p$ with increasing field above H_c.

In order to understand the true nature of the magnetic transitions of TbNi$_5$, we have recently performed high resolution powder neutron diffraction study of TbNi$_5$ and found new magnetic satellites, which were not seen previously and we interpreted as the evidence of a modulated magnetic structure [12]. We have described our new results in terms of a fan-like structure with two wave vectors ($\mathbf{k}_1 = 0$ and $\mathbf{k}_2 \approx (2\pi/c)(0,\ 0,\ 0.019)$). In this model, the magnetic moments of Tb-ions have mutually orthogonal ferromagnetic (μ_f) and modulated (μ_{mod}) basal-plane components. The magnetic satellites of our neutron diffraction pattern were observed over the whole temperature region of 2 ∼ 23 K in contrast with the original explanation of Ref. [11]. Moreover, we did not observe a clear anomaly in the temperature dependence of the intensities of both ferromagnetic peaks and satellites at 16.5 K, where a ferromagnet – helimagnet transition is expected to occur according to Refs. [10, 11]. It should also be mentioned that in our previous studies [12] we did not investigate the effects of external magnetic field on the magnetic structure of $TbNi_5$ although the field dependence of the magnetic structure may be important to understand better the experimental observations of Refs. [10, 11].

Although our previous high-resolution powder diffraction studies elucidated some interesting aspect of the magnetic transition, however in order to have full understanding of it we need additional detailed and careful studies of the magnetic structure of $TbNi_5$ using a single crystal sample and especially its field dependence. Therefore, we have performed neutron diffraction experiments on a $TbNi_5$ single crystal at temperatures of $2 \sim 30$ K under magnetic fields. The measurements were carried out while both heating and cooling. Besides, we made AC susceptibility, magnetization, and heat capacity measurements in order to compare the bulk properties of our single crystal with the results published earlier [9 – 11].

2. Experimental details. Our $TbNi_5$ alloy was prepared from high-purity starting materials in an induction furnace using an Al_2O_3 crucible under argon atmosphere. Subsequent heat treatment of the alloy was made at 1100 °C for 8 hours. The single crystal was then cut out from a grain of an ingot and subsequently ground to a sphere of approximate 2 mm diameter. The remaining part of the ingot was used for heat capacity measurements and powder X-ray diffraction studies, confirming the single-phase structure of $CaCu_5$ type. The lattice parameters were determined as $a = 4.8986(4)$ and $c = 3.9606(4)$ Å at room temperature.

Rocking curves (ω-scans) around the (100), (001), (101), and (002) reflections were measured with the double-axis E-4 diffractometer at the BENSC, Hahn-Meitner Institute. The incident neutron wavelength was 2.44 Å. The (002) reflection with a large nuclear intensity was used for the intermittent check of the orientation of the sample while varying temperature or/and magnetic field. A horizontal magnetic field was applied along the a- or c-axes. The data analysis was done using the FULLPROF package [13].

The magnetization and AC susceptibility of the single crystal were taken by using a SQUID-magnetometer at the Institute of Metal Physics of RAS. The AC susceptibility was measured in an alternating field of 10 Oe at a frequency of 90 Hz. The specific heat was studied by a PMC device at Paul Scherrer Institute.

3. Experimental results and discussion. Fig.1 shows the thermal variation of the real and imaginary parts of the AC susceptibility measured with field parallel to the a-axis of the $TbNi_5$ single crystal. The temperature dependence of the heat capacity is also presented in Fig.1c for both cooling and heating curves. All the data exhibit a distinct maximum at $T \approx 23$ K that evidences an order – disorder transition. On the other hand, we note that the imaginary susceptibility has another anomaly at $T \approx 8$ K.

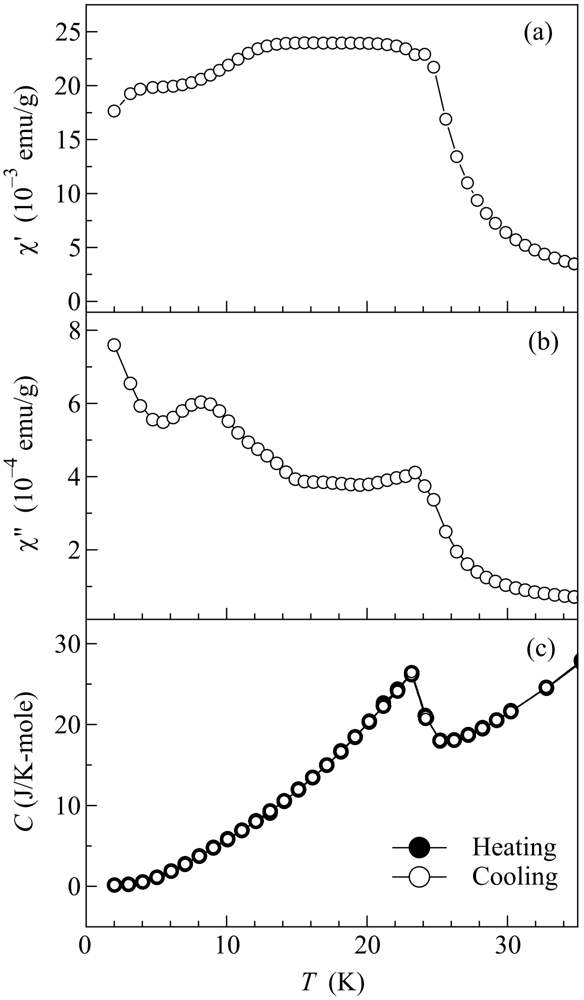

Fig.1. Temperature dependence of (a) real and (b) imaginary parts of AC susceptibility and (c) heat-capacity, measured while heating (closed symbols) and cooling (open symbols)

Fig.2 shows the neutron diffraction data scanned around the (001) reflection while cooling from room temperature to 2 K. The (001) reflection is a pure nuclear peak at temperatures above 25 K. The magnetic contributions to the (001) reflection and the $(001)^{\pm}$ magnetic satellites begin to appear at $T_p = 24$ K and their in-

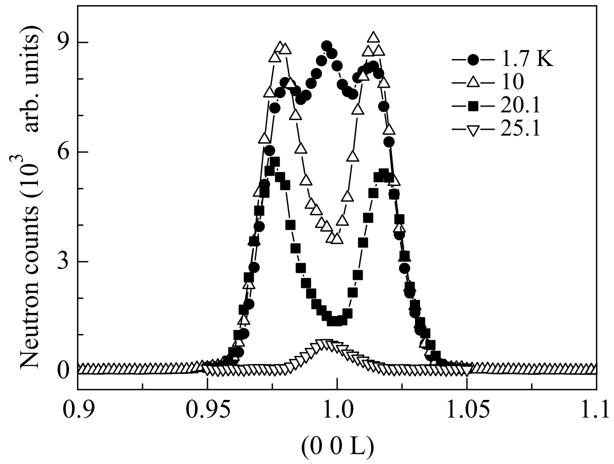

Fig.2. Neutron diffraction spectra around (0 0 1) reflection scanning along [0 0 L] direction taken at (●)1.7, (△)10.0, (■)20.1 and (▽)25.1 K while cooling

tensities increase upon cooling down to $T_f^c \approx 10$ K. A further cooling to 7 K produces a sharp increase of the (001) reflection intensity and simultaneous decrease of both satellites. This behavior is clearly seen from the temperature dependence of the integrated intensities of the (001) reflection and the $(001)^{\pm}$ satellites shown in Fig.3. Similar curves were also obtained for the (100) and (101) reflections as well as their $(100)^{\pm}$ and $(101)^{\pm}$ satellites.

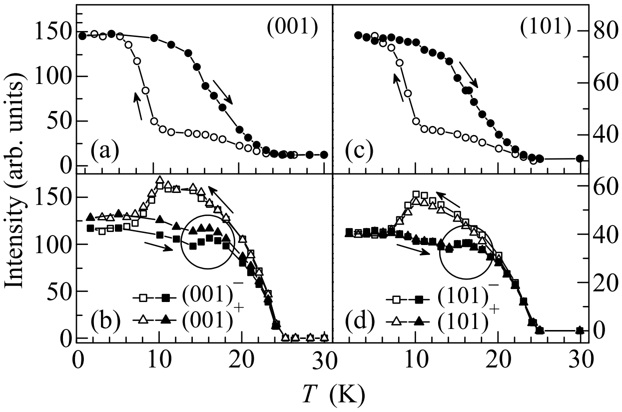

Fig.3. Temperature dependence of the integrated intensities of (a) (001) and (c) (101) reflections and (b) $(001)^{\pm}$ and (d) $(101)^{\pm}$ satellites. Open and closed symbols are for data taken while cooling and heating, respectively. Squares and triangles are for minus and plus satellites, respectively

Upon heating, there is a relatively slow decrease of the intensities of the (100), (001), (101) reflections and $(100)^{\pm}$, $(001)^{\pm}$, $(101)^{\pm}$ satellites over the region of 2.2 ~ 14 K before they all decrease sharply at the temperatures of 16 ~ 23 K (see Fig.3). However, the main reflections and satellites exhibit different behavior over the temperature region of 14 ~ 16 K: the main reflections decrease continuously with temperature while the satellites increase slightly as marked by the circles in Figs.3b and 3d. A comparison of the heating and cooling curves of the intensities shows clearly the existence of large thermal hysteresis.

A similar hysteresis is also observed in the temperature dependence of the wave vector $\mathbf{k}_2$. We determined $\mathbf{k}_2$ from the distance between the positions of $(101)^{\pm}$ satellites, and the results are presented in Fig.4. As one can see in the figure, the $\mathbf{k}_2$ vector has different values for the heating and cooling curves at $T > 10$ K. Below 10 K the wave vector becomes almost the same for both curves within the resolutions of our experiments with $\mathbf{k}_2 \approx (2\pi/c)0.0181$, indicating that a lock-in transition occurs at $T \simeq 10$ K.

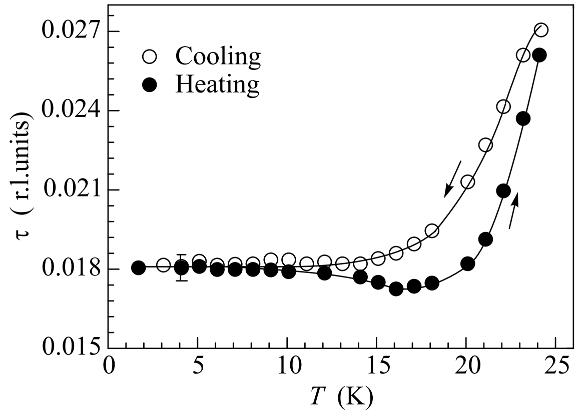

Fig.4. Temperature dependence of the wave vector $\mathbf{k}_2$

Thus, the TbNi$_5$ compound undergoes two magnetic transitions. One is the order-disorder type transition at $T_p = (24 \pm 1)$ K for both cooling and heating. When the temperature decreases, a low-temperature transition is observed at $T_f^c \approx 10$ K as a sharp change in the intensities of the main reflections and satellites. One of the features of this low-temperature transition is the large thermal hysteresis, evidence of the first order transition. Taking into account the temperature dependence of $\mathbf{k}_2$ vector below 10 K, we speculate that a lock-in structure occurs at $T < 10$ K; its wave vector is estimated to be $\mathbf{k}_2 \approx (2\pi/c)0.0181 \approx 1/55$ r.l.u. (reciprocal lattice units) below 10 K.

We believe that the most probable source of the transition at T_f^c is the magnetic anisotropy of Tb ions. When the temperature decreases the magnetic anisotropy increases and tends to orient the magnetic moments of Tb ions along the easy direction (the a-axis). This causes the increase of the a-axis ferromagnetic component (μ_f, parallel to the a axis) and simultaneously the decrease of the modulated one (μ_{mod}, perpendicular to the a-axis) over the temperature interval of 7 ~ 10 K. The changes of μ_f and μ_{mod} below 10 K are calculated from the (101) reflection intensity and we have obtained $\Delta\mu_f = 1.9\,\mu_B$ and $\Delta\mu_{\mathrm{mod}} = -1.3\,\mu_B$, respectively. The value of the total magnetic moment of Tb ion remains almost the same as expected in this temperature range.

Another feature of the low-temperature transition is the absence of a clear anomaly in the thermal variation of the heat capacity at T_f^c (see Fig.1). A similar behavior was previously found in the cooling measurements of some of RGa_2 compounds [14]. An absence of such a peak in the heat capacity data implies that there is a very small difference between the free energies of the two magnetic phases above and below T_f^c. In such a case, one can expect that small magnetic field can transform the modulated phase into the ferromagnetic one.

In fact, it is exactly what we found in our field measurements. Fig.5 shows the scans measured around the (101) reflection under magnetic fields. Magnetic fields were applied along the a-axis at 2 K. It is clearly seen in Fig.5 that the magnetic field suppresses the satellites significantly and induces a collinear ferromagnetic state at $\mu_0 H_c \approx 3.5$ kOe. Interestingly enough, with increasing magnetic field not the position but the intensity of the satellite peaks changes. It should be mentioned too that the induced ferromagnetic state remains stable even when the external field is switched off (see Fig.6). As one can see from the insert of Fig.6, the Tb-ion magnetic moment reaches the value of $\mu_f = 7.3 \pm 0.1\,\mu_B$ at the field-induced ferromagnetic state. This value is in good agreement with the results of the magnetic measurements. However, the critical field value H_c determined by us is larger by a factor of 8 than that found in Ref. [11]. It is not clear to us at the moment what causes such a big difference in the two estimates of H_c values.

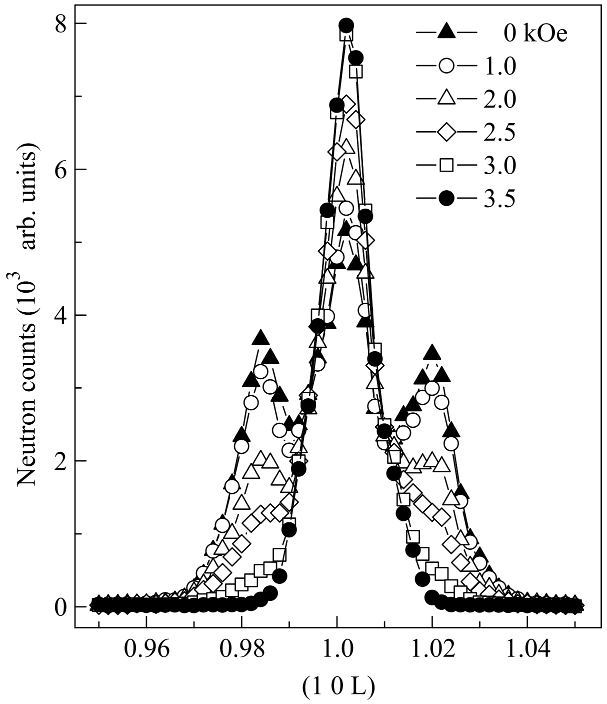

Fig.5. Neutron spectra around the (1 0 1) reflection scanning along the [0 0 L] direction at 2 K by varying magnetic fields

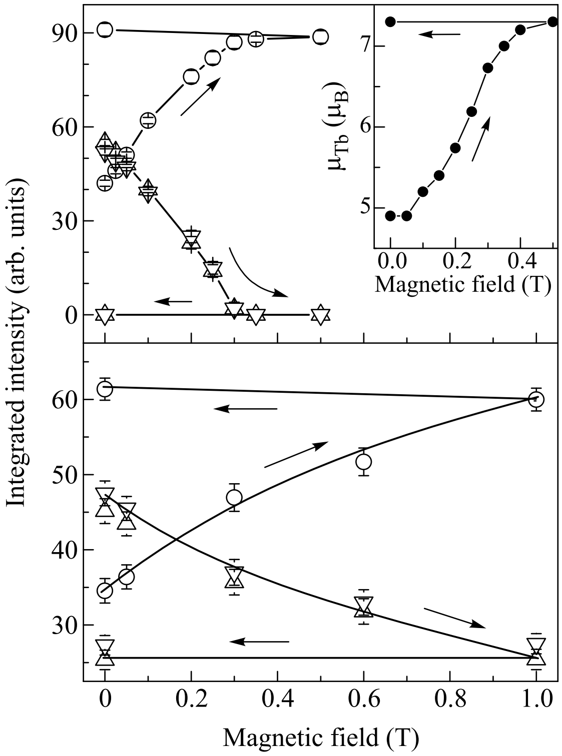

Fig.6. Field dependence of the integrated intensities of the (101) reflection (circles) and $(101)^{\pm}$ satellites (up and down triangles) at (top) 2 K and (bottom) 10 K. The field was applied along the a-axis at 2 K and along the c-axis at 10 K. Insert shows the field dependence of the ferromagnetic component of the Tb-ion magnetic moment obtained at 2 K

The aforementioned increase of the (101) reflection intensity by an external field is an expected and natural result because a magnetic field was applied along the easy magnetization direction. What is surprising is, however, that the intensity increases even when a magnetic field is applied along the hard magnetization direction (i.e. the c-axis). It is clearly seen from the bottom part of Fig.6, where the field dependence of the (101) reflection and $(101)^{\pm}$ are presented for field applied to the c-axis at 10 K. In a simple case the (101) intensity should decrease with increasing field along the c-axis, because field tends to rotate a magnetic moment to the c-axis and, therefore, decreases a moment projected to the scattering plane. In our case the (101) intensity increases when a field increases to the maximal value of 10 kOe. Furthermore, the field-induced magnetic state remains stable even after fields were switched off. Thus, an external field for any direction transforms the modulated magnetic structure to the collinear ferromagnetic one; which is very unusual.

Taking into account our data, we can now understand the yet unexplained results of μSR measurements [7]. It was found that the temperature dependence of a damping rate exhibits a jump near 15 K when a crystal was heated. Our results presented here indicate that the decrease of the ferromagnetic component may cause the observed jump in the μSR damping rate.

4. Conclusion. On the base of our results, we can conclude that two spontaneous transitions occur in $TbNi_5$ compound. One ($T_p = 24\,\text{K}$) is the second order transition from the paramagnetic state to the incommensurate structure. Another one ($T_f^c = 10\,\text{K}$) is the first order transition from the incommensurate structure to the lock-in structure. The external magnetic field of $\mu_0 H_c \approx 3.5\,\text{kOe}$ is enough to transform irreversibly the modulated structure to the collinear ferromagnetic one. All these results indicate that the modulated structure is weakly stable against magnetic field.

We are grateful for the hospitality at BENSC HMI. Financial support was provided by project RFBR-Ural # 04-02-96082p2004. A. Pirogov acknowledges the support of the CSCMR through the SRC program of KOSEF of Korea. Works at Sungkyunkwan University was supported by the CNRF project of the KAERI.

---

1. J. J. France and R. J. Radwanski, Ferromagnetic Materials Vol. 7, Ed. K. H. J. Buschow (North-Holland, Amsterdam, 1993) p. 307.
2. D. Gignoux, A. Nait-Saada, and R. Perrier de la Bäthie, J. Phys. (Paris) C5 **40**, 188 (1979).
3. P. Svoboda, J. Vejpravova, N.-T. H. Kim-Ngan, and F. Kaysel, J. Magn. Magn. Mat. **272-276**, 595 (2004).
4. R. Lemaire and D. Paccard, C. R. Acad. Sci Paris **270**, 1131 (1970).
5. E. A. Goremychkin, E. Muehle, P. G. Ivanitskii et al., Phys. Status Solidi B **121**, 623 (1984).
6. D. Gignoux and J. J. Rhyne, J. Magn. Magn. Mat. **54-57**, 1267 (1986).
7. P. Dalmas de Réotier, A. Yaouanc, P. C. M. Gubbens et al., J. Magn. Magn. Mat. **104-107**, 1267 (1992).
8. C. Carboni, D. Gignoux, and A. Tari, Phys. Rev. B **52**, 9486 (1995).
9. J. A. Blanco, D. Gignoux, D. Schmitt et al., J. Phys.: Condens. Mat. **6**, 4335 (1994).
10. V. M. T. Barthem and E. A. M. da Gamma, J. Phys.: Condens. Mat. **9**, 7609 (1997).
11. V. M. T. Barthem, H. S. Amorim, D. Schmit, and D. Gignoux, J. Magn. Magn. Mat. **208**, 97 (2000).
12. Seongsu Lee, A. N. Pirogov, J.-G. Park et al., Europhys. Lett. **63**, 350 (2003).
13. J. Rodriguez-Carvajal, Physica B **192**, 55 (1993).
14. A. R. Ball, D. Gignoux, and D. Schmitt. J. Magn. Magn. Mat. **119**, 96 (1993).